Eur. Phys. J. C 48, 401–411 (2006)
DOI 10.1140/epjc/s10052-006-0029-1

THE EUROPEAN PHYSICAL JOURNAL C

Regular Article – Theoretical Physics

Large strong phases and CP violation in the annihilation processes $\bar{B}^0 \to K^+K^-$, $K^{*\pm}K^{\mp}$, $K^{*+}K^{*-}$

F. Su[1,2], Y.-L. Wu[1,a], Y.-D. Yang[3], C. Zhuang[1,2]

[1] Institute of Theoretical Physics, Chinese Academy of Science, Beijing 100080, P.R. China
[2] Graduate School of the Chinese Academy of Science, Beijing 100039, P.R. China
[3] Department of Physics, Henan Normal University, Xinxiang, Henan 453007, P.R. China

Received: 17 April 2006 / Revised version: 6 July 2006 /
Published online: 24 October 2006 –

Abstract. The strong phases and CP violation in the rare $\bar{B}^0 \to K^+K^-$, $K^{*\pm}K^{\mp}$, $K^{*+}K^{*-}$ decays are investigated. As these decays proceed only via annihilation type diagrams in the standard model (SM), a dynamical gluon mass is introduced to avoid the infrared divergence in the soft endpoint regions. The Cutkosky rule is adopted to deal with a physical-region singularity of the on-mass-shell quark propagators, which leads to a big imaginary part and hence a large strong phase. As a consequence, large CP asymmetries are predicted in those decay modes due to a big interference between the annihilation amplitudes from penguin and tree operators, which may be tested in future more precise experiments.

PACS. 13.25.Hw; 11.30.Er; 12.38.Bx

1 Introduction

Charmless B-meson decays are of crucial importance to deepen our insights into the flavor structure of the standard model (SM), the origin of CP violation, the dynamics of hadronic decays, and to search for any signals of new physics beyond the SM. CP violation, as an important part of B physics, has been paid much attention to in recent years. Both mixing-induced and direct CP violations have been observed in the neutral B meson decays [1–5], which has provided a new window for exploring the origin and mechanism of CP violation after the establishment of indirect and direct CP violations in kaon decays [6–13]. The possible implications of charmless B decays and their large CP violation have been investigated in recent papers [14–20]. In the SM, the only source of CP violation in the SM is the single Kobayashi–Maskawa phase [21] in the mixing matrix that describes the charged current weak interaction of quarks. However, physics beyond the SM is usually associated with new sources of CP violation. For instance, rich sources of CP violation can be induced from a single relative phase of the vacuum in the simple two Higgs doublet model with spontaneous CP violation (S2HDM or type III 2HDM) [22–25]. This model can provide a natural explanation for the CP violation in the SM and also lead to a new type of CP-violating source with each quark and lepton carrying a non-trivial CP-violating phase. Therefore, explorations of CP violation may well indicate physics beyond the SM, or may be very helpful to distinguish between various realizations of one particular kind of new physics after the corresponding new physics particles have been observed directly.

In addition to serving as a tool of looking for any new physics, studying of CP violation can also be used to test various factorization hypotheses, such as the "naive" factorization approach (FA) [26–29], the QCD factorization (QCDF) [30, 31], and the perturbation QCD method (pQCD) [32–34].

These methods have very different understandings of the hadronic B-meson decays. For the FA method, it cannot predict the direct CP asymmetries properly due to the assumption of no strong re-scattering in the final states; the pQCD generally predicts large strong phases and big direct CP violations. Furthermore, in this approach it is also believed that annihilation diagrams are important in non-leptonic two-body B-meson decays [35, 36]; while the QCDF favors small direct CP violations in general because of the α_s-suppressed strong phases.

It is known that, in most cases of two-body B-meson decays, the weak annihilation contribution carries different weak and strong phases for the tree and penguin amplitudes, which is very important for studying CP-violating observables. Meanwhile, the calculation of annihilation contributions is interesting by itself, since it can help us to understand the low energy dynamics of QCD involved in heavy meson decays and the viability

[a] e-mail: ylwu@itp.ac.cn

of the theoretical approaches mentioned above. Motivated by these arguments, we shall investigate in this paper the pure annihilation processes $\bar{B}^0 \to K^+K^-$, $K^{*\pm}K^{\mp}$, $K^{*+}K^{*-}$. These decay channels have some interesting features.

Firstly, they are all pure annihilation processes and studying these decay modes in the SM can serve as a probe for the annihilation strength in hadronic B-meson decays. Secondly, the current experimental data on the decay $\bar{B}^0 \to K^+K^-$ [37] has already provided direct evidence for the existence of the annihilation contributions. By comparing our theoretical result for the branching ratio of the decay $\bar{B}^0 \to K^+K^-$ with the experimental data, we can test the feasibility of the theoretical method and get a deeper insight into the penguin annihilation and the W-exchanged topologies in the $B \to \pi\pi, \pi K$ decay modes [20, 38]. Thirdly, their strong phases are calculable and found to be big, which leads to large CP violation. The resulting branching ratios for $\mathcal{B}(\bar{B}^0 \to K^+K^-)$ is consistent with the current experimental data [37]. Finally, studying the polarization in the $\bar{B}^0 \to K^{*+}K^{*-}$ decay may also help us to clarify whether annihilation contribution could resolve or alleviate the polarization puzzles in $B \to \phi K^*$ decays as suggested in [39].

In calculating the hard-scattering kernel, we shall use the Cornwall [40–42] prescription of the gluon propagator by introducing a dynamical gluon mass to avoid enhancements in the soft endpoint region. It is interesting to note that recent theoretical [43–49] and phenomenological [50–52] studies are now accumulating support for a softer infrared behavior for the gluon propagator. Moreover, we will adopt the Cutkosky rule [53] to deal with the physical-region singularity caused by the on-mass-shell quark propagators, which then produce big imaginary parts from the kinematic region where the virtual quark becomes on-mass-shell. By applying these two "tricks", we observe that the main contributions to the decay amplitudes come from the non-factorizable diagrams, and the CP-averaged branching ratios of $\bar{B}^0 \to K^+K^-, K^+K^{*-}, K^-K^{*+}$, and $K^{*+}K^{*-}$ are estimated using QCD factorization to be about 2.02×10^{-8}, 4.23×10^{-8}, 5.70×10^{-8}, and 6.89×10^{-8} for a given gluon mass $m_g = 500\,\mathrm{MeV}$, respectively. Moreover, big strong phases are predicted in these decay modes, and hence the direct and mixing-induced CP violations C_{KK} and S_{KK} are found to be very large in these decays as the differences ΔC_{KK} and ΔS_{KK} are small in $\bar{B}^0 \to K^{\pm}K^{*\mp}$ decays. The predictions may be tested in the more precise experiments at the B-factory and the LHC-b.

The paper is organized as follows. In Sect. 2, we first analyze the relevant Feynman diagrams and then outline the necessary ingredients for evaluating the CP asymmetries of the $\bar{B}^0 \to K^+K^-$, $K^{*\pm}K^{\mp}$, $K^{*+}K^{*-}$ decays. In Sect. 3, we present the approaches for dealing with the physical-region singularities of gluon and quark propagators. The numerical results of the CP-averaged branching ratios and large strong phases are given in Sect. 4. Finally, we discuss the CP asymmetries for those decay modes and give conclusions in Sects. 5 and 6, respectively. The necessary input parameters and the complete decay amplitudes for those decay modes are given in the appendixes.

2 Rephase-invariant CP-violating observables

Using the operator product expansion and renormalization group equation, the low energy effective Hamiltonian for charmless two-body B-meson decays can be written as [54]

$$\mathcal{H}_{\rm eff} = \frac{G_{\rm F}}{\sqrt{2}} \left\{ V_{ub}V_{ud}^*[C_1(\mu)O_1(\mu) + C_2(\mu)O_2(\mu)] - V_{tb}V_{td}^* \sum_{i=3}^{10} C_i(\mu)O_i(\mu) \right\} + \text{h.c.}\,, \tag{1}$$

where $C_i(\mu)$ $(i = 1, \ldots, 10)$ are the Wilson coefficient functions which have been reliably evaluated to next-to-leading logarithmic order. The effective operators O_i are defined as follows:

$$\begin{aligned}
O_1 &= \left(\bar{d}_i u_i\right)_{V-A} \left(\bar{u}_j b_j\right)_{V-A}\,, \\
O_2 &= \left(\bar{d}_i u_j\right)_{V-A} \left(\bar{u}_j b_i\right)_{V-A}\,, \\
O_3 &= \left(\bar{d}_i b_i\right)_{V-A} \sum_q \left(\bar{q}_j q_j\right)_{V-A}\,, \\
O_4 &= \left(\bar{d}_i b_j\right)_{V-A} \sum_q \left(\bar{q}_j q_i\right)_{V-A}\,, \\
O_5 &= \left(\bar{d}_i b_i\right)_{V-A} \sum_q \left(\bar{q}_j q_j\right)_{V+A}\,, \\
O_6 &= \left(\bar{d}_i b_j\right)_{V-A} \sum_q \left(\bar{q}_j q_i\right)_{V+A}\,, \\
O_7 &= \frac{3}{2}\left(\bar{d}_i b_i\right)_{V-A} \sum_q e_q \left(\bar{q}_j q_j\right)_{V+A}\,, \\
O_8 &= \frac{3}{2}\left(\bar{d}_i b_j\right)_{V-A} \sum_q e_q \left(\bar{q}_j q_i\right)_{V+A}\,, \\
O_9 &= \frac{3}{2}\left(\bar{d}_i b_i\right)_{V-A} \sum_q e_q \left(\bar{q}_j q_j\right)_{V-A}\,, \\
O_{10} &= \frac{3}{2}\left(\bar{d}_i b_j\right)_{V-A} \sum_q e_q \left(\bar{q}_j q_i\right)_{V-A}\,.
\end{aligned} \tag{2}$$

Here i and j are $SU(3)$ color indices, q denotes all the active quarks at the scale $\mu = \mathcal{O}(m_b)$, i.e., $q = u, d, s, c, b$.

With the effective Hamiltonian, calculations of the leading order amplitudes for $\bar{B}^0 \to K^+K^-$, $K^{*\pm}K^{\mp}$, $K^{*+}K^{*-}$ decays are straightforward. However, due to the conservation of the vector current and partial conservation of the axial-vector current, the leading order amplitudes will vanish in the limit $m_u, m_s \to 0$. In order to probe the annihilation strength and discuss CP violation in these processes, we have to consider the next-to-leading order ($\alpha_{\rm s}$ order) contributions.

Up to the $\alpha_{\rm s}$ order, the relevant Feynman diagrams contributing to the $\bar{B}^0 \to K^+K^-$ decay (the corresponding diagrams for the $K^{*\pm}K^{\mp}$ and $K^{*+}K^{*-}$ modes are the same)

are depicted in Fig. 1 (corresponding to the W-exchanged annihilation diagrams) and Fig. 2 (corresponding to the penguin annihilation diagrams and including the case with the exchange of $u \leftrightarrow s$). For the factorizable diagrams a and b in Figs. 1 and 2, their contributions cancel each other both in the W-exchanged and in the penguin annihilation diagrams, so that the non-factorizable contributions will dominate the decay, which can be obtained by calculating the amplitudes of diagrams c and d in Figs. 1 and 2. Moreover, it is noted that these properties hold in all of these decay modes.

The direct CP violation occurs only if there are two contributing amplitudes with non-zero relative weak and strong phases. The weak phase difference can arise from the interference of amplitudes from various tree (current–current) and penguin diagrams. From the Feynman diagrams in Figs. 1 and 2, we can see that in these decays there are two kinds of CKM elements, $V_{ub}V_{ud}^*$ from tree operators and $V_{tb}V_{td}^*$ from penguin ones, which will induce weak phase difference and hence CP violation. The total decay amplitudes for the $B^0(\bar{B}^0) \to K^+K^-$ mode can be written as

$$\begin{aligned}\mathcal{A}(B^0 \to K^+K^-) &= V_{ub}^*V_{ud}\mathcal{A}_{\rm T} - V_{tb}^*V_{td}\mathcal{A}_{\rm P} \\ &= V_{ub}^*V_{ud}\mathcal{A}_{\rm T}[1 + z\mathrm{E}^{\mathrm{i}(\alpha+\delta)}]\,, \qquad (3)\\ \mathcal{A}(\bar{B}^0 \to K^+K^-) &= V_{ub}V_{ud}^*\mathcal{A}_{\rm T} - V_{tb}V_{td}^*\mathcal{A}_{\rm P} \\ &= V_{ub}V_{ud}^*\mathcal{A}_{\rm T}[1 + z\mathrm{E}^{\mathrm{i}(-\alpha+\delta)}]\,, \qquad (4)\end{aligned}$$

where $\alpha = \arg[-V_{tb}^*V_{td}/V_{ub}^*V_{ud}]$, $z = |V_{tb}^*V_{td}/V_{ub}^*V_{ud}|$ $|\mathcal{A}_{\rm P}/\mathcal{A}_{\rm T}|$, which indicates the interference strength between the annihilation amplitudes from penguin and tree operators, and $\delta = \arg(\mathcal{A}_{\rm P}/\mathcal{A}_{\rm T})$ is the relative strong phase between the penguin and the tree annihilation amplitudes. A similar consideration can be applied to the $B^0 \to K^{\pm}K^{*\mp}$ and $B^0 \to K^{*+}K^{*-}$ decays. The resulting decay amplitudes by using QCD factorization are given in Appendix B. For neutral B-meson decays, the time-dependent CP asymmetries are defined as

$$\mathcal{A}_{CP}(t) = \frac{\Gamma(B^0(t) \to f) - \Gamma(\bar{B}^0(t) \to \bar{f})}{\Gamma(B^0(t) \to f) + \Gamma(\bar{B}^0(t) \to \bar{f})}\,. \qquad (5)$$

When the final state is a CP eigenstate, such as the $B^0(\bar{B}^0) \to K^+K^-$ decay, the time-dependent CP asymmetries can be written as

$$\mathcal{A}_{CP}(t) = C_{KK}\cos(\Delta m t) + S_{KK}\sin(\Delta m t)\,, \qquad (6)$$

where Δm is the mass difference of the two eigenstates of the B_d mesons. C_{KK} and S_{KK} are parameters describing the direct and the mixing-induced CP violation, respectively. Both of them depend on the CKM and hadronic matrix elements

$$C_{KK} = \frac{1 - |\lambda_{CP}|^2}{1 + |\lambda_{CP}|^2}\,, \quad S_{KK} = \frac{-2\,\mathrm{Im}(\lambda_{CP})}{1 + |\lambda_{CP}|^2}\,, \qquad (7)$$

with

$$\lambda_{CP} = \frac{V_{tb}^*V_{td}\langle K^+K^-|H_{\rm eff}|\bar{B}^0\rangle}{V_{tb}V_{td}^*\langle K^+K^-|H_{\rm eff}|B^0\rangle}\,. \qquad (8)$$

From (3) and (4), the CP-violating parameters C_{KK} and S_{KK} can be expressed explicitly as

$$\begin{aligned}C_{KK} &= \frac{-2z\sin\alpha\sin\delta}{1 + 2z\cos\alpha\cos\delta + z^2}\,,\\ S_{KK} &= \frac{-\sin 2\alpha - 2z\sin\alpha\cos\delta}{1 + 2z\cos\alpha\cos\delta + z^2}\,, \qquad (9)\end{aligned}$$

which shows that both the direct and the mixing-induced CP violation depend not only on the strong phase δ but also on the magnitudes of z. Thus, when the contributions of different weak decay amplitudes are comparable to each other, there will be a high likelihood for observable CP-violating asymmetries.

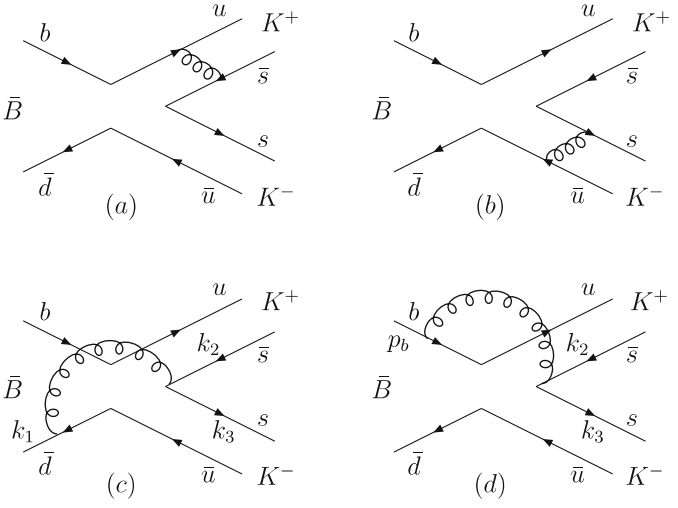

Fig. 1. The W-exchanged annihilation diagrams for $\bar{B}^0 \to K^+K^-$ decay

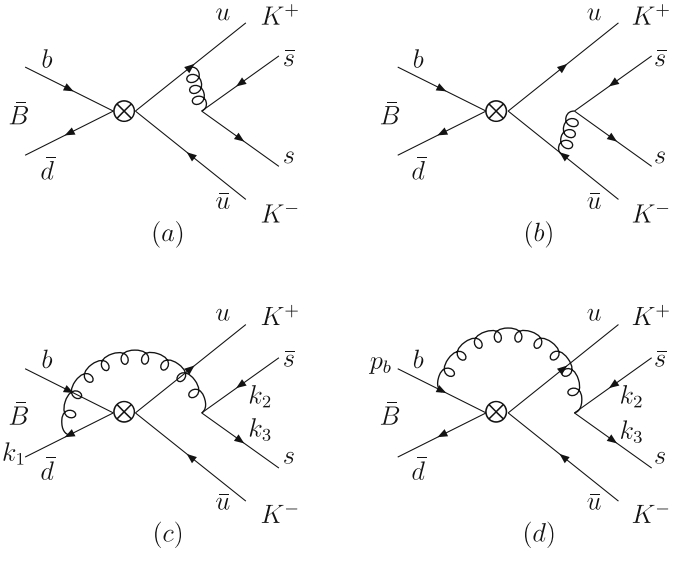

Fig. 2. The penguin annihilation diagrams for $\bar{B}^0 \to K^+K^-$ decay

For the case of $B \to K^{*\pm}K^{\mp}$ decays, as the final state is not an CP eigenstate, the CP-violating asymmetries become complicated. There are in general four decay amplitudes which can be expressed as

$$g = \langle K^+K^{*-}|H_{\rm eff}|B\rangle\,, \quad h = \langle K^+K^{*-}|H_{\rm eff}|\bar{B}\rangle\,,$$
$$\bar{g} = \langle K^-K^{*+}|H_{\rm eff}|\bar{B}\rangle\,, \quad \bar{h} = \langle K^-K^{*+}|H_{\rm eff}|B\rangle\,. \quad (10)$$

Following the discussions in [55], there exist in general four rephase-invariant parameters $a_{\varepsilon'}$, $a_{\bar{\varepsilon}'}$, $a_{\varepsilon+\varepsilon'}$, $a_{\varepsilon+\bar{\varepsilon}'}$ which characterize the CP asymmetries. We may redefine the following four parameters:

$$C_{KK} = \frac{1}{2}(a_{\varepsilon'} + a_{\bar{\varepsilon}'})\,, \qquad \Delta C_{KK} = \frac{1}{2}(a_{\varepsilon'} - a_{\bar{\varepsilon}'})\,,$$
$$S_{KK} = \frac{1}{2}(a_{\varepsilon+\varepsilon'} + a_{\varepsilon+\bar{\varepsilon}'})\,, \quad \Delta S_{KK} = \frac{1}{2}(a_{\varepsilon+\varepsilon'} - a_{\varepsilon+\bar{\varepsilon}'})\,, \quad (11)$$

with

$$a_{\bar{\varepsilon}'} = \frac{|g|^2 - |h|^2}{|g|^2 + |h|^2}\,, \qquad a_{\bar{\varepsilon}'} = \frac{|\bar{h}|^2 - |\bar{g}|^2}{|\bar{h}|^2 + |\bar{g}|^2}\,,$$
$$a_{\varepsilon+\varepsilon'} = \frac{-2\,{\rm Im}(h/g)}{1+|h/g|^2}\,, \quad a_{\varepsilon+\bar{\varepsilon}'} = \frac{-2\,{\rm Im}(\bar{g}/\bar{h})}{1+|\bar{g}/\bar{h}|^2}\,. \quad (12)$$

For a final state being a CP eigenstate, one has $\Delta C_{KK} = 0$ and $\Delta S_{KK} = 0$.

As for the $B \to K^{*+}K^{*-}$ decay mode, since the total amplitudes are dominated by the longitudinal ones, which can be seen below, one can evaluate its CP asymmetries in the same way as for the $B \to K^+K^-$ decay.

3 Treatments for physical-region singularities of gluon and quark propagators

To perform a numerical calculation, the QCD factorization approach may be used to evaluate the amplitudes of $\bar{B}^0 \to K^+K^-$, $K^{*\pm}K^{\mp}$, $K^{*+}K^{*-}$ decays. The details are presented in Appendix B. In (B.3)–(B.8), one will encounter the endpoint divergence, which is the most difficult part to deal with in the annihilation diagrams within the QCD factorization framework. Instead of the widely used treatment $\int_0^1 \frac{{\rm d}y}{y} \to X_A = (1+\varrho_A {\rm E}^{{\rm i}\varphi}) \ln \frac{m_B}{\Lambda_h}$ in the literature [56–60], we shall use an effective gluon propagator [40–42, 61, 62] to treat the infrared divergence in the soft endpoint region:

$$\frac{1}{k^2} \Rightarrow \frac{1}{k^2 + M_{\rm g}^2(k^2)}\,, \quad M_{\rm g}^2(k^2) = m_g^2 \left[\frac{\ln\left(\frac{k^2+4m_g^2}{\Lambda^2}\right)}{\ln\left(\frac{4m_g^2}{\Lambda^2}\right)}\right]^{-\frac{12}{11}}. \quad (13)$$

The typical values $m_g = (500 \pm 200)$ MeV, and $\Lambda = \Lambda_{\rm QCD} = 250$ MeV will be taken in our numerical calculations. Use of this gluon propagator is supported by the lattice [63] and the field theoretical studies [43–49], which have shown that the gluon propagator is not divergent as fast as $\frac{1}{k^2}$.

After giving the treatments for the infrared divergence arising from the gluon propagator, we now turn to show how to deal with a physical-region singularity of the on-mass-shell quark propagators. It can be easily checked that each Feynman diagram contributing to a given matrix element is entirely real unless some denominators vanish with a physical-region singularity, so that the iε prescription for treating the poles becomes relevant. In other words, a Feynman diagram will yield an imaginary part for decay amplitudes when the virtual particles in the diagram become on-mass-shell; thus, the diagram may be considered as a genuine physical process. The Cutkosky rules [53] give a compact expression for the discontinuity across the cut arising from a physical-region singularity. When applying the Cutkosky rules to deal with a physical-region singularity of quark propagators, the following formula holds:

$$\frac{1}{(k_1-k_2-k_3)^2 + {\rm i}\varepsilon} = P\left[\frac{1}{(k_1-k_2-k_3)^2}\right] - {\rm i}\pi\delta[(k_1-k_2-k_3)^2]\,, \quad (14)$$

$$\frac{1}{(p_b-k_2-k_3)^2 - m_b^2 + {\rm i}\varepsilon} = P\left[\frac{1}{(p_b-k_2-k_3)^2 - m_b^2}\right] - {\rm i}\pi\delta\left[(p_b-k_2-k_3)^2 - m_b^2\right]\,, \quad (15)$$

where P denotes the principal-value prescription. The role of the δ function is to put the particles corresponding to the intermediate state on their positive energy mass-shell, so that in the physical region, the individual diagrams satisfy the unitarity condition. Equations (14) and (15) will be applied to the quark propagators D_d and D_b in (B.3)–(B.8), respectively. It is then seen that the big imaginary parts arise from the virtual quarks (d, b) across their mass-shells as physical-region singularities. In fact, the above imaginary parts are among the main sources of strong phases for the $\bar{B}^0 \to K^+K^-$, $K^{*\pm}K^{\mp}$, $K^{*+}K^{*-}$ decays as discussed in the perturbative QCD approach [36, 64].

4 Decay amplitudes and large strong phases

Using the relevant input parameters listed in Appendix A, we can calculate the tree and the penguin annihilation amplitudes for each decay mode and their corresponding numerical results for the quantities z and δ, which are presented in Table 1. With these considerations, the CP-averaged branching ratios for these decay modes are given in Table 2. In this table, we present our "default results" along with detailed error estimates corresponding to the different theoretical uncertainties listed in Appendix A. The first error refers to the variation of the dynamical gluon mass, while the second one refers to the uncertainty due to the CKM parameters A, λ, $\bar{\rho}$, and $\bar{\eta}$. Finally, the last error originates from the uncertainty due to the meson decay constants and the parameter μ_K.

From the numerical results given in Tables 1 and 2, we arrive at the following observations.

Table 1. The tree annihilation amplitudes $\mathcal{A}_{\rm T}$, the penguin annihilation amplitudes $\mathcal{A}_{\rm P}$, magnitudes of z and the strong phase δ for $B^0(\bar{B}^0) \to K^+K^-, K^{*\pm}K^{\mp}, K^{*+}K^{*-}$ decays. Here we give only the case when $m_g = 500\,\text{MeV}$

Decay mode	$\mathcal{A}_{\rm T}$	$\mathcal{A}_{\rm P}$	z	δ
$B^0(\bar{B}^0) \to K^+K^-$	$0.0273 - 0.0321\text{i}$	$-0.0114 + 0.0045\text{i}$	0.65	-153°
$B^0(\bar{B}^0) \to K^-K^{*+}$	$0.0467 - 0.0371\text{i}$	$0.0187 - 0.0005\text{i}$	0.70	37°
$B^0(\bar{B}^0) \to K^+K^{*-}$	$0.0412 - 0.0464\text{i}$	$0.0333 - 0.0092\text{i}$	1.14	33°
$B^0(\bar{B}^0) \to K^{*+}K^{*-}$	$0.0634 - 0.0543\text{i}$	$-0.0168 + 0.0047\text{i}$	0.47	-155°

Table 2. The CP-averaged branching ratios (in units of 10^{-8}) of the $B^0(\bar{B}^0) \to K^+K^-$, $K^{*\pm}K^{\mp}$, $K^{*+}K^{*-}$ decays. The *theoretical errors shown from left to right* correspond to the uncertainties referred to as "gluon mass", "CKM parameters", and "decay constants and the parameter μ_K" as specified in the text

Decay mode	Br	$\Gamma_{\rm T}/\Gamma$	Exp.
$B^0(\bar{B}^0) \to K^+K^-$	$2.02^{+3.21+0.83+1.01}_{-0.81-0.54-0.44}$	–	$(4 \pm 15 \pm 8) \times 10^{-8}$ [37]
$B^0(\bar{B}^0) \to K^-K^{*+}$	$5.70^{+2.08+2.26+1.11}_{-3.01-1.71-0.92}$	–	–
$B^0(\bar{B}^0) \to K^+K^{*-}$	$4.23^{+2.29+1.63+0.94}_{-2.05-1.21-0.81}$	–	–
$B^0(\bar{B}^0) \to K^{*+}K^{*-}$	$6.89^{+1.78+2.87+2.04}_{-1.50-2.19-1.58}$	0.01	$< 1.41 \times 10^{-4}$ [65]

– The strong phase associated with the tree amplitude $\mathcal{A}_{\rm T}$ is about $\delta \simeq -45^\circ$, while the imaginary part of the penguin amplitude $\mathcal{A}_{\rm P}$ is comparatively small; moreover, from the numerical results of the magnitude z, we can see that the penguin annihilation amplitudes are comparable to the tree ones, so that a large interference effect between the tree and the penguin annihilation amplitudes occurs. Combining these two ingredients, it is expected that there exist large CP violations in these decay modes, which will be shown below.

– For a given dynamical gluon mass, the CP-averaged branching ratios of these decay modes follow the pattern

$$\begin{aligned}\mathcal{B}(\bar{B}^0 \to K^{*+}K^{*-}) &> \mathcal{B}(\bar{B}^0 \to K^{*\pm}K^{\mp}) \\ &> \mathcal{B}(\bar{B}^0 \to K^+K^-)\,, \end{aligned} \quad (16)$$

which is due to the larger vector-meson decay constant $f_{K^*} > f_K$ for one vector meson in the final state or the larger spin phase space available for two final-state vector mesons.

– For the $\bar{B}^0 \to K^+K^-$ decay, the presently obtained result is consistent with the experimental data [37], and also in agreement with the one given in [56]: $\mathcal{B}(\bar{B}^0 \to K^+K^-) = (0.013^{+0.005+0.008+0.087}_{-0.005-0.005-0.011}) \times 10^{-6}$, when considering the huge uncertainties caused in the treatment of infrared divergence $\int_0^1 \frac{\mathrm{d}y}{y} \to X_A = (1 + \varrho_A \mathrm{E}^{\mathrm{i}\varphi}) \ln \frac{m_B}{\Lambda_h}$. The present theoretical errors mainly originate from the variation of the dynamical gluon mass, while our theoretical result alleviates the dependence of the input parameters when compared to the one given by [56]. Another significant error comes from the parameter μ_K, as the decay amplitudes include the μ_K^2 factor when considering the twist-three wave function contributions. Moreover, the present central value is smaller than the one given by pQCD [66]: $\mathrm{Br}(B^0 \to K^+K^-) = 4.6 \times 10^{-8}$, which has used a bigger parameter μ_K. If we also choose $\mu_K = 2.22\,\text{GeV}$, just as pQCD does, and a dynamical gluon mass with $m_g = 420\,\text{MeV}$, we can get the same result as the pQCD prediction. Namely, if choosing smaller μ_K, to get the same result as the pQCD prediction, one has to choose a smaller m_g. In general, with the parameter μ_K fixed at the value 1.4, 1.8 and 2.2 GeV, we can get the same result as the pQCD by taking m_g to be $m_g = 340, 370$, and 420 MeV, respectively. Anyway, our prediction is consistent with the pQCD result after taking into account the theoretical uncertainties.

– For the $\bar{B}^0 \to K^{\pm}K^{*\mp}$ decays, from the numerical results we can see that the main theoretical errors originate from dynamical gluon mass and CKM parameters. In addition, we predict that $\mathcal{B}(\bar{B}^0 \to K^+K^{*-}) \neq \mathcal{B}(\bar{B}^0 \to K^-K^{*+})$. The central values are larger than the ones given in [56]: $\mathcal{B}(\bar{B}^0 \to K^{\pm}K^{*\mp}) = (0.014^{+0.007+0.010+0.106}_{-0.006-0.006-0.012}) \times 10^{-6}$, but they remain consistent with each other within the uncertainties.

– For the $\bar{B}^0 \to K^{*+}K^{*-}$ decay, only an upper limit at 90% confidence level has been reported [65]:

$$\mathcal{B}(\bar{B}^0 \to K^{*+}K^{*-}) < 1.41 \times 10^{-4}\,. \quad (17)$$

Obviously, the present numerical result is far below the experimental data. It is noted that the branching ratio of this decay channel is less sensitive to the dynamics gluon mass, and the theoretical errors mainly come from the CKM parameters. It is also noted that 99% of the branching ratio comes from the longitudinal

part, and the result is consistent with that given by the pQCD method [67].

5 Large CP violation

We now turn to a discussion of the CP asymmetries in the $B^0(\bar{B}^0) \to K^+K^-, K^{*\pm}K^{\mp}, K^{*+}K^{*-}$ decays. As there are big strong phases and large interference effects in these decay modes, large CP-violating asymmetries are expected. It is very reasonable to neglect the transverse contribution and consider only the longitudinal part in $\bar{B}^0 \to K^{*+}K^{*-}$ decay, since the transverse polarization fraction provides only a 1% contribution to the total branching ratio of this mode. Thus we can discuss the CP asymmetries in the K^+K^- and $K^{*+}K^{*-}$ decay modes in the same manner.

Using the relevant formulas provided in the previous section, we are able to calculate the CP violations in the $\bar{B}^0 \to K^+K^-, K^{*\pm}K^{\mp}, K^{*+}K^{*-}$ decays. Firstly, in Table 3, we present our predictions for the rephase-invariant CP-violating observables and their theoretical errors in these decays. Secondly, taking the CKM angle α as a free parameter, the dependence of the CP-violating parameters on the angle α is shown in Figs. 3 and 4.

From Table 3 and Figs. 3 and 4 we come to the following observations.

(i) For the $\bar{B}^0 \to K^+K^-$ decay, due to the large strong phase δ and the large magnitude $z \simeq 0.65$, the direct and mixing-induced CP-violating parameters C_{KK} and S_{KK} are found to be quite large. The direct CP asymmetry is consistent with the one given by pQCD [66]. It is also seen that the CP asymmetry parameters C_{KK} and S_{KK} are not sensitive to the choice of the dynamical gluon mass, and the main theoretical errors originate from the CKM parameters.

Table 3. The CP asymmetries for the $B^0(\bar{B}^0) \to K^+K^-, K^{*\pm}K^{\mp}, K^{*+}K^{*-}$ decays with the same error resources as in Table 2

mode	C_{KK}	ΔC_{KK}	S_{KK}	ΔS_{KK}
K^+K^-	$0.39^{+0.00+0.04+0.01}_{-0.04-0.04-0.01}$	0.00	$0.86^{+0.09+0.04+0.02}_{-0.05-0.08-0.05}$	0.00
$K^{\pm}K^{*\mp}$	$-0.59^{+0.11+0.05+0.01}_{-0.00-0.07-0.01}$	$0.01^{+0.00+0.01+0.01}_{-0.04-0.01-0.01}$	$-0.74^{+0.29+0.02+0.06}_{-0.12-0.08-0.04}$	$-0.07^{+0.08+0.06+0.06}_{-0.08-0.06-0.06}$
$K^{*+}K^{*-}$	$0.30^{+0.02+0.05+0.00}_{-0.01-0.05-0.00}$	0.00	$0.78^{+0.01+0.09+0.00}_{-0.01-0.10-0.00}$	0.00

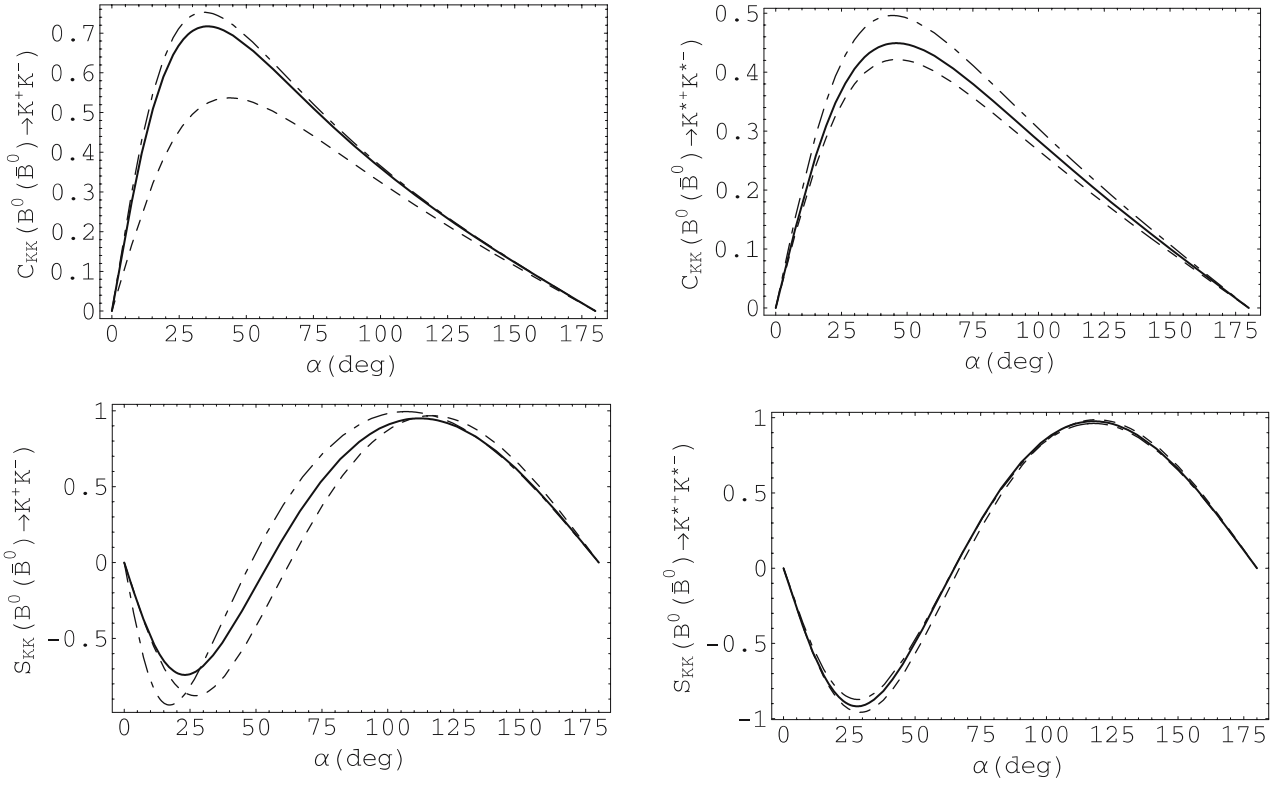

Fig. 3. The CP violation parameters C_{KK} and S_{KK} for the $B^0(\bar{B}^0) \to K^+K^-, K^{*+}K^{*-}$ decays as functions of the weak phase α (in degrees). The *dash-dotted*, *solid*, and *dashed lines* correspond to $m_g = 300$ MeV, 500 MeV, and 700 MeV, respectively

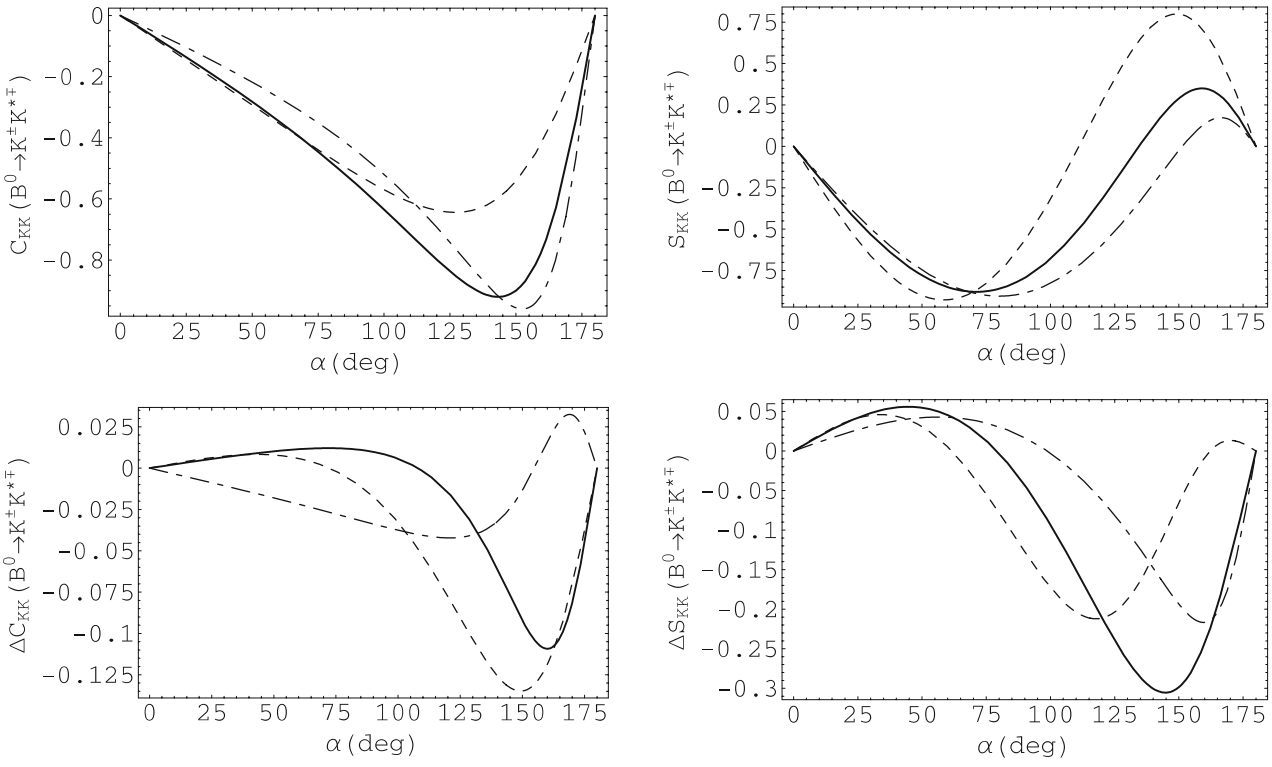

Fig. 4. The same as Fig. 3, but for the $B^0(\bar{B}^0) \to K^{\pm}K^{*\mp}$ decays

(ii) For the $\bar{B}^0 \to K^{*+}K^{*-}$ decay, as it is dominated by the longitudinal part, the CP asymmetries in this decay mode have the same manner as the one in the $\bar{B}^0 \to K^+K^-$ decay. Thus we arrive at the similar conclusions as the ones for the $\bar{B}^0 \to K^+K^-$ decay.

(iii) In contrast to the $\bar{B}^0 \to K^+K^-$, $K^{*+}K^{*-}$ decays, the strong phases δ in the $\bar{B}^0 \to K^{\pm}K^{*\mp}$ decay modes have opposite signs, so that the sign of the CP asymmetry parameter C_{KK} is also opposite to the ones in the $K^+K^-, K^{*+}K^{*-}$ decay modes. In addition, the rephase-invariant parameters C_{KK} and S_{KK} in the $\bar{B}^0 \to K^{\pm}K^{*\mp}$ decay modes also characterize large CP violation as the parameters ΔC_{KK} and ΔS_{KK} are small. Note that only the mixing-induced CP violation S_{KK} is sensitive to the dynamical gluon mass.

(iv) It is seen from Figs. 3 and 4 that all CP-violating parameters have a strong dependence on the weak angle α. So these observables may be used to determine the range of the angle α in future more precise experiments.

6 Conclusions

In summary, we have calculated the strong phases, the CP-averaged branching ratios, and the CP asymmetries for the pure annihilation decays $\bar{B}^0 \to K^+K^-, K^{\pm}K^{*\mp}$, and $K^{*+}K^{*-}$ within the standard model. It has been shown that the non-factorizable contributions dominate these decays, and the contributions of the penguin diagrams are comparable to that of the W-exchanged diagrams; the CP-averaged branching ratios of these decay modes are at the order of $10^{-8} \sim 10^{-7}$, and these small branching ratios predicted in the SM make them sensitive to any new physics beyond the SM. In particular, as there are big strong phases and large interference effects between the tree and the penguin annihilation amplitudes, the CP-violating parameters C_{KK} and S_{KK} have been predicted to be large in these decay modes. It has been seen that the CP-violating parameters have a strong dependence on the weak phase α, but they are not sensitive to the dynamical gluon mass except the mixing-induced CP violation in the $\bar{B}^0 \to K^{*+}K^-, K^+K^{*-}$ decays. The resulting branching ratio $\mathrm{Br}(\bar{B}^0 \to K^+K^-)$ is consistent with the current experimental data. It is then expected that the predicted CP asymmetries should be reasonable.

In this paper, we have adopted the Cornwall prescription for the gluon propagator with a dynamical mass to avoid the endpoint infrared divergence. Note that when the intrinsic mass is appropriately introduced, it may not spoil the gauge symmetry as shown recently in the symmetry-preserving loop regularization [68, 69]. Meanwhile, we have also applied the Cutkosky rules to deal with the physical-region singularity of the on-mass-shell quark propagators. As a consequence, it produces big imaginary parts which are very important for understanding large CP violations. The combination of the two treatments for the endpoint infrared divergence of the gluon propagator and the physical-region singularity of the quark propagators enables us to obtain, by using the QCD factorization approach [30, 31],

reasonable results which are consistent with the ones [66, 67] obtained by using the perturbative QCD approach[32–34]. However, this is different from the treatment of a perturbative QCD approach where the Sudakov factors have been used to avoid the endpoint divergence. As a consequence, it was shown that the pQCD predictions are insensitive to the choice of Sudakov factors and to the dependence of the impact parameter b [35].

It is noted that our present predictions for the branching ratios depend on the dynamics gluon mass which plays the role of IR cut-off; such a dependence should in general be matched from the non-perturbative effects in the transition wave functions. However this is not the case in general for direct CP violation. With the experimental and theoretical improvements, this quantity could be fitted from a well measured pure annihilation decay mode and then expanded to other decays. In order to check the validity of the gluon-mass regulator method adopted to deal with the endpoint divergence, we plan to extend this method to the vertex corrections and hard spectator interactions for other charmless B-meson decays. We expect that these corrections are independent of the dynamical gluon mass, which is under investigation. Anyhow, the treatment presented in this paper may enhance its predictive power for analyzing the charmless non-leptonic B-meson decays.

Acknowledgements. This work was supported in part by the National Science Foundation of China (NSFC) under the grant 10475105, 10491306, and the Project of Knowledge Innovation Program (PKIP) of Chinese Academy of Sciences.

Appendix A: Input parameters

The theoretical predictions in our calculations depend on many input parameters, such as the Wilson coefficient functions, the CKM matrix elements, the hadronic parameters, and so on. We present all the relevant input parameters as follows.

The next-to-leading order Wilson coefficient functions (at $\mu = m_b/2$) in the NDR scheme for γ_5 [60] have been used with the following numerical values:

$$\begin{aligned} &C_1 = 1.130\,, && C_2 = -0.274\,, && C_3 = 0.021\,,\\ &C_4 = -0.048\,, && C_5 = 0.010\,, && C_6 = -0.061\,,\\ &C_7 = -0.005/128\,, && C_8 = 0.086/128\,, &&\\ &C_9 = -1.419/128\,, && C_{10} = 0.383/128\,. && \end{aligned} \tag{A.1}$$

For the B meson wave function, we have taken the following results [70, 71]:

$$\Phi_1^B(\bar{\rho}) = N_B \bar{\rho}^2(1-\bar{\rho})^2 \exp\left[-\frac{1}{2}\left(\frac{\bar{\rho} m_B}{\omega_B}\right)^2\right], \tag{A.2}$$

with $\omega_B = 0.25\,\mathrm{GeV}$, and N_B being a normalization constant. For the light-cone wave functions of the light mesons, we use the asymptotic form as given in [72–74]:

$$\begin{aligned} &\Phi_K(u) = \Phi_\parallel(u) = \Phi_\perp(u) = 6u\bar{u}\,, && \text{twist-2 LCDAs}\,,\\ &\phi_\sigma(u) = g_\perp^{(a)}(u) = h_\parallel^{(s)}(u) = 6u\bar{u}\,,&&\\ &g_\perp^{(v)}(u) = \frac{3}{4}\left[1+(u-\bar{u})^2\right]\,,&&\\ &h_\parallel^{(t)}(u) = 3-12u\bar{u}\,, \quad \phi_k(u) = 1\,, && \text{twist-3 LCDAs}\,, \end{aligned} \tag{A.3}$$

with $\bar{u} = 1-u$.

For the other parameters used in our calculations, we give a list as follows [65]:

$$\begin{aligned} M_{B_d} &= 5.28\,\mathrm{GeV}\,, & m_b &= 4.66\,\mathrm{GeV}\,,\\ M_{K^{*\pm}} &= 0.89\,\mathrm{GeV}\,, & \tau_{B_d^0} &= 1.536\,\mathrm{ps}\,,\\ f_{B_d} &= 200\pm 30\,\mathrm{MeV}\,, & f_K &= 160\,\mathrm{MeV}\,,\\ f_{K^*} &= 218\pm 4\,\mathrm{MeV}\,, & f_{K^*}^\perp &= 175\pm 25\,\mathrm{MeV}\,,\\ V_{ud} &= 1-\lambda^2/2\,, & V_{ub} &= A\lambda^3(\rho-\mathrm{i}\eta)\,,\\ V_{td} &= A\lambda^3(1-\rho-\mathrm{i}\eta)\,, & V_{tb} &= 1\,. \end{aligned} \tag{A.4}$$

The Wolfenstein parameters of the CKM matrix elements are taken as [65] $A = 0.8533 \pm 0.0512$, $\lambda = 0.2200 \pm 0.0026$, $\bar{\rho} = 0.20 \pm 0.09$, $\bar{\eta} = 0.33 \pm 0.05$, with $\bar{\rho} = \rho(1-\frac{\lambda^2}{2})$, $\bar{\eta} = \eta(1-\frac{\lambda^2}{2})$. The coefficient of the twist-three distribution amplitude of the pseudoscalar K meson is chosen as $\mu_K = \mu_\pi = 1.5 \pm 0.2\,\mathrm{GeV}$ [30, 31, 56].

Appendix B: The decay amplitudes

To evaluate the hadronic matrix elements, we may adopt the QCD factorization formalism. For the annihilation process $\bar{B} \to M_1M_2$, the matrix element can be written as [56]

$$\langle M_1M_2|O_i|\bar{B}^0\rangle = f_B\Phi_B * f_{M_1}\Phi_{M_1} * f_{M_2}\Phi_{M_2} * T_i\,, \tag{B.1}$$

where O_i is the effective operator appearing in the effective weak Hamiltonian, the $*$ products imply integrations over the light-cone momentum fractions of the constituent quarks inside the relevant mesons. T_i is the hard-scattering kernel that can be computed perturbatively with the QCD factorization approach. Φ_M and f_i are the leading-twist light-cone distribution amplitudes and the decay constants, respectively.

Using (B.1) and the meson wave functions given in [70–74], we can evaluate the decay amplitudes of the W-exchanged diagrams in Fig. 1 (only the O_1 operator has a contribution) and the penguin annihilation diagrams in Fig. 2 (O_4, O_6, O_8, and O_{10} have contributions).

For final states containing two pseudoscalar K meson, the amplitudes are found to be

$$\begin{aligned} &\mathcal{A}_\mathrm{T}(\bar{B}_d \to K^+K^-) = C_1A_1\,,\\ &\mathcal{A}_\mathrm{P}(\bar{B}_d \to K^+K^-) = \left(2C_4+\frac{C_{10}}{2}\right)A_1 + \left(2C_6+\frac{C_8}{2}\right)A_2\,, \end{aligned} \tag{B.2}$$

where

$$A_1 = \frac{G_{\rm F}}{\sqrt{2}} f_B f_K^2 \pi\alpha_s(\mu) \frac{C_F}{N_C^2} \int_0^1 {\rm d}\xi \int_0^1 {\rm d}x \int_0^1 {\rm d}y \Phi_1^B(\xi)$$
$$\times \left\{ \left(x\frac{M_B^4}{D_d k^2} + (y+\xi-\xi_B)\frac{M_B^4}{D_b k^2} \right) \Phi_k(x)\Phi_k(y) \right.$$
$$+ \frac{\mu_K^2}{M_B^2} \left[\left((x+y-\xi)\phi_k(x)\phi_k(y) \right.\right.$$
$$+ (y-\xi-x)\phi_k(x)\frac{\phi'_\sigma(y)}{6} - (y-\xi-x)\phi_k(y)\frac{\phi'_\sigma(x)}{6}$$
$$\left. -(x+y-\xi)\frac{\phi'_\sigma(x)\phi'_\sigma(y)}{36} \right) \frac{M_B^4}{D_d k^2}$$
$$+ \left((x+y+\xi-2\xi_B)\phi_k(x)\phi_k(y) \right.$$
$$+ (y+\xi-x)\phi_k(x)\frac{\phi'_\sigma(y)}{6} - (y+\xi-x)\phi_k(y)\frac{\phi'_\sigma(x)}{6}$$
$$\left.\left. +(x+y+\xi-2)\frac{\phi'_\sigma(x)\phi'_\sigma(y)}{36} \right) \frac{M_B^4}{D_b k^2} \right] \right\}, \qquad \text{(B.3)}$$

$$A_2 = \frac{G_{\rm F}}{\sqrt{2}} f_B f_K^2 \pi\alpha_s(\mu) \frac{C_F}{N_C^2} \int_0^1 {\rm d}\xi \int_0^1 {\rm d}x \int_0^1 {\rm d}y \Phi_1^B(\xi)$$
$$\times \left\{ \left((y-\xi)\frac{M_B^4}{D_d k^2} + (x-\xi_B)\frac{M_B^4}{D_b k^2} \right) \Phi_k(x)\Phi_k(y) \right.$$
$$+ \frac{\mu_K^2}{M_B^2} \left[\left((x+y-\xi)\phi_k(x)\phi_k(y) \right.\right.$$
$$- (y-\xi-x)\phi_k(x)\frac{\phi'_\sigma(y)}{6} + (y-\xi-x)\phi_k(y)\frac{\phi'_\sigma(x)}{6}$$
$$\left. -(x+y-\xi)\frac{\phi'_\sigma(x)\phi'_\sigma(y)}{36} \right) \frac{M_B^4}{D_d k^2}$$
$$+ \left((x+y+\xi-2\xi_B)\phi_k(x)\phi_k(y) \right.$$
$$- (y+\xi-x)\phi_k(x)\frac{\phi'_\sigma(y)}{6} + (y+\xi-x)\phi_k(y)\frac{\phi'_\sigma(x)}{6}$$
$$\left.\left. +(x+y+\xi-2)\frac{\phi'_\sigma(x)\phi'_\sigma(y)}{36} \right) \frac{M_B^4}{D_b k^2} \right] \right\}, \qquad \text{(B.4)}$$

where $\xi_B = (M_B - m_b)/M_B$, with M_B being the mass of the B_d meson, $\phi'_\sigma(x) = \frac{{\rm d}\phi_\sigma(x)}{{\rm d}x}$, and the Φ's and ϕ's are the leading-twist (twist-two) and twist-three light-cone distribution amplitudes of mesons, respectively. We set the scale μ to be the averaged virtuality of the time-like gluon, i.e., $\mu = m_b/2$. k^2 and $D_{b,d}$ arise from the propagators of the virtual gluon, the bottom quark b, and the down quark d, respectively.

For $\bar{B}_d \to K^{\pm}K^{*\mp}$ decays, we need only consider the longitudinal wave function of the vector K^* meson, due to the conservation of the angular momentum. The corresponding decay amplitudes of $\bar{B}_d \to K^+K^{*-}$ are given in the same form as (B.2), but with the amplitudes of A_1 and A_2 replaced by

$$A_1 = \frac{G_{\rm F}}{\sqrt{2}} f_B f_K \pi\alpha_s(\mu) \frac{C_F}{N_C^2} \int_0^1 {\rm d}\xi \int_0^1 {\rm d}x \int_0^1 {\rm d}y \Phi_1^B(\xi)$$
$$\times \left[f_{K^*} \left(x\frac{M_B^4}{D_d k^2} + (y+\xi-\xi_B)\frac{M_B^4}{D_b k^2} \right) \Phi_k(x)\Phi_k(y) \right.$$
$$+ f_{K^*}^{\perp}\mu_K \frac{m_{K^*}}{M_B} \left((-x+y-\xi)\frac{h_\parallel^{\prime(s)}(y)\phi'_\sigma(x)}{12} \right.$$
$$- (x+y-\xi)\frac{h_\parallel^{\prime(s)}(y)\phi(x)}{2} + (x+y-\xi)\frac{\phi'_\sigma(x)h_\parallel^{(t)}(y)}{3}$$
$$\left. +2(x-y+\xi)\phi(x)h_\parallel^{(t)}(y) \right) \frac{M_B^4}{D_d k^2}$$
$$+ f_{K^*}^{\perp}\mu_K \frac{m_{K^*}}{M_B} \left((-x+y-\xi)\frac{h_\parallel^{\prime(s)}(y)\phi'_\sigma(x)}{12} \right.$$
$$- (x+y+\xi-2\xi_B)\frac{h_\parallel^{\prime(s)}(y)\phi(x)}{2}$$
$$- (x+y+\xi-2)\frac{\phi'_\sigma(x)h_\parallel^{(t)}(y)}{3}$$
$$\left. \left. +(x-y-\xi)\phi(x)h_\parallel^{(t)}(y) \right) \frac{M_B^4}{D_b k^2} \right], \qquad \text{(B.5)}$$

$$A_2 = \frac{G_{\rm F}}{\sqrt{2}} f_B f_K \pi\alpha_s(\mu) \frac{C_F}{N_C^2} \int_0^1 {\rm d}\xi \int_0^1 {\rm d}x \int_0^1 {\rm d}y \Phi_1^B(\xi)$$
$$\times \left[f_{K^*} \left((-y+\xi)\frac{M_B^4}{D_d k^2} + (x+\xi_B)\frac{M_B^4}{D_b k^2} \right) \Phi_k(x)\Phi_k(y) \right.$$
$$+ f_{K^*}^{\perp}\mu_K \frac{m_{K^*}}{M_B} \left((-x+y-\xi)\frac{h_\parallel^{\prime(s)}(y)\phi'_\sigma(x)}{12} \right.$$
$$+ (x+y-\xi)\frac{h_\parallel^{\prime(s)}(y)\phi(x)}{2} - (x+y-\xi)\frac{\phi'_\sigma(x)h_\parallel^{(t)}(y)}{3}$$
$$\left. +2(x-y+\xi)\phi(x)h_\parallel^{(t)}(y) \right) \frac{M_B^4}{D_d k^2}$$
$$+ f_{K^*}^{\perp}\mu_K \frac{m_{K^*}}{M_B} \left((-x+y-\xi)\frac{h_\parallel^{\prime(s)}(y)\phi'_\sigma(x)}{12} \right.$$
$$+ (x+y+\xi-2\xi_B)\frac{h_\parallel^{\prime(s)}(y)\phi(x)}{2}$$
$$+ (x+y+\xi-2)\frac{\phi'_\sigma(x)h_\parallel^{(t)}(y)}{3}$$
$$\left. \left. +(x-y-\xi)\phi(x)h_\parallel^{(t)}(y) \right) \frac{M_B^4}{D_b k^2} \right], \qquad \text{(B.6)}$$

where $h_\parallel^{\prime(s)}(y) = \frac{{\rm d}h_\parallel^{(s)}(y)}{{\rm d}y}$. With the change for the signs of the second and the third terms in the twist-three amplitudes in (B.5) and (B.6) and the exchange of the variable x and y of the wave functions, we can get the corresponding decay amplitudes of $\bar{B}_d \to K^-K^{*+}$ mode.

Finally, for the $\bar{B} \to K^{*+}K^{*-}$ decay, in the rest frame of the $\bar{B}^0$ system, we have $\lambda_1 = \lambda_2 = \lambda$ (where λ_1 and λ_2 denote the helicities of the K^{*+} and K^{*-} mesons, respectively) through the helicity conservation, since the $\bar{B}^0$ me-

son has helicity zero. So, there are generally three decay amplitudes, H_0, H_+, and H_-, representing $\lambda = 0$, 1, and -1, respectively. Considering only the leading-twist contributions, we can get the longitudinal amplitudes $\mathcal{A}_{0T}$ and $\mathcal{A}_{0P}$ of the decay $\bar{B}_d \to K^{*+}K^{*-}$ from (B.3) and (B.4) by keeping only the $\Phi_k(x)\Phi_k(y)$ term and replacing the decay constant f_K by f_{K^*}. The total longitudinal amplitude is then given as

$$H_0 = V_{ub}V_{ud}^*\mathcal{A}_{0T} - V_{tb}V_{td}^*\mathcal{A}_{0P}\,. \tag{B.7}$$

As for the transverse amplitude $H_\pm$, we have

$$\begin{aligned}
H_+ = {} & \frac{G_{\rm F}}{\sqrt{2}} f_B f_{K^*}^\perp \frac{m_{K^*}^2}{M_B^2}\pi\alpha_s(\mu)\frac{C_F}{N_C^2} \\
& \times \int_0^1 \mathrm{d}\xi \int_0^1 \mathrm{d}x \int_0^1 \mathrm{d}y \Phi_1^B(\xi) \left(C_1 + 2C_4 + \frac{C_{10}}{2}\right) \\
& \times \left(\left(-f(x) g_\perp^{(v)}(y) - g_\perp^{(v)}(x) g_\perp^{(a)}(y)/4 \right.\right. \\
& \left. + f(x) g_\perp^{\prime(a)}(y)/8 + g_\perp^{\prime(a)}(x) g_\perp^{(a)}(y)/32 \right) \frac{M_B^4}{D_d k^2} \\
& + \left(-f(x) g_\perp^{(v)}(y) + g_\perp^{(v)}(x) g_\perp^{(a)}(y)/4 \right. \\
& \left.\left. - f(x) g_\perp^{\prime(a)}(y)/8 + g_\perp^{\prime(a)}(x) g_\perp^{(a)}(y)/32 \right) \frac{M_B^4}{D_b k^2} \right) \\
& + \frac{G_{\rm F}}{\sqrt{2}} f_B f_{K^*}^\perp \frac{m_{K^*}^2}{M_B^2}\pi\alpha_s(\mu)\frac{C_F}{N_C^2} \\
& \times \int_0^1 \mathrm{d}\xi \int_0^1 \mathrm{d}x \int_0^1 \mathrm{d}y \Phi_1^B(\xi) \left(2C_6 + \frac{C_8}{2}\right) \\
& \times \left(\left(-g_\perp^{(v)}(x) f(y) + g_\perp^{(a)}(x) g_\perp^{(v)}(y)/4 \right.\right. \\
& \left. - g_\perp^{\prime(a)}(x) f(y)/8 + g_\perp^{(a)}(x) g_\perp^{\prime(a)}(y)/32 \right) \frac{M_B^4}{D_d k^2} \\
& + \left(-g_\perp^{(v)}(x) f(y) - g_\perp^{(a)}(x) g_\perp^{(v)}(y)/4 \right. \\
& \left.\left. + g_\perp^{\prime(a)}(x) f(y)/8 + g_\perp^{(a)}(x) g_\perp^{\prime(a)}(y)/32 \right) \frac{M_B^4}{D_b k^2} \right)\,,
\end{aligned} \tag{B.8}$$

where the function $f(x) = \int_0^x \mathrm{d}u \left(\phi_\parallel(u) - g_\perp^{(v)}(u)\right)$ and $g_\perp^{\prime(a)}(y) = \frac{\mathrm{d}g_\perp^{(a)}(y)}{\mathrm{d}y}$. Changing the signs of the $g_\perp^{(a)} g_\perp^{(v)}$ and $g_\perp^{\prime(a)} f$ terms in (B.8), we can get the other amplitude, H_-.

References

1. BaBar Collaboration, B. Aubert et al., Phys. Rev. Lett. **87**, 091 801 (2001)
2. Bell Collabration, K. Abe et al., Phys. Rev. Lett. **87**, 091 802 (2001)
3. Belle Collaboration, K. Abe et al., Phys. Rev. Lett. **93**, 021 601 (2004)
4. BaBar Collaboration, B. Aubert et al., Phys. Rev. Lett. **93**, 131 801 (2004)
5. Belle Collaboration, Y. Chao et al., Phys. Rev. Lett. **93**, 191 802 (2004)
6. J.H. Christenson, J.W. Cronin, V.L. Fitch, R. Turlay, Phys. Rev. Lett. **13**, 138 (1964)
7. NA48 Collaboration, J.R. Batley et al., Phys. Lett. B **544**, 97 (2002)
8. KTeV Collaboration, A. Alavi-Harati et al., Phys. Rev. D **67**, 012 005 (2003)
9. Y.L. Wu, Phys. Rev. D **64**, 016 001 (2001)
10. Y.L. Wu, Intern. Conf. on Flavor Physics (ICFP2001), ed. by Y.-L. Wu (World Scientific Pub. Co., 2001), pp. 217–236
11. Y.L. Wu, Int. J. Mod. Phys. A **7**, 2863 (1992)
12. J. Heinrich, E.A. Paschos, J.M. Schwarz, Y.L. Wu, Phys. Lett. B **279**, 140 (1992)
13. Y.L. Wu, ICHEP92 (Dallas, 1992), p. 506
14. A.J. Buras et al., Phys. Rev. Lett. **92**, 101 804 (2004)
15. T. Yoshikawa, Phys. Rev. D **68**, 054 023 (2003)
16. D. Atwood, G. Hiller, hep-ph/0307251
17. S. Mishima, T. Yoshikawa, hep-ph/0408090
18. S. Nandi, A. Kundu, hep-ph/0407061
19. Y.L. Wu, Y.F. Zhou, Phys. Rev. D **71**, 021 701 (2005)
20. Y.L. Wu, Y.F. Zhou, Phys. Rev. D **72**, 034 037 (2005)
21. M. Kobayashi, T. Maskawa, Prog. Theor. Phys. **49**, 652 (1973)
22. Y.L. Wu, CMU-Report, hep-ph/9404241 (1994)
23. Y.L. Wu, L. Wolfenstein, Phys. Rev. Lett. **73**, 1762 (1994)
24. L. Wolfenstein, Y.L. Wu, Phys. Rev. Lett. **73**, 2809 (1994)
25. Y.L. Wu, Y.F. Zhou, Phys. Rev. D **61**, 096 001 (2000)
26. M. Wirbel, B. Stech, M. Bauer, Z. Phys. C **29**, 637 (1985)
27. M. Bauer, B. Stech, M. Wirbel, Z. Phys. C **34**, 103 (1987)
28. L.L. Chau, H.Y. Cheng, W.K. Sze, H. Yao, B. Tseng, Phys. Rev. D **43**, 2176 (1991)
29. L.L. Chau, H.Y. Cheng, W.K. Sze, H. Yao, B. Tseng, Phys. Rev. D **58**, 019 902 (1998)
30. M. Beneke, G. Buchalla, M. Neubert, C.T. Sachrajda, Phys. Rev. Lett. **83**, 1914 (1999)
31. M. Beneke, G. Buchalla, M. Neubert, C.T. Sachrajda, Nucl. Phys. B **579**, 313 (2000)
32. H.N. Li, H.L. Yu, Phys. Rev. Lett. **74**, 4388 (1995)
33. H.N. Li, H.L. Yu, Phys. Lett. B **353**, 301 (1995)
34. Y.Y. Keum, H.N. Li, A.I. Sanda, Phys. Rev. D **63**, 054 008 (2001)
35. Y.Y. Keum, H.N. Li, A.I. Sanda, Phys. Lett. B **504**, 6 (2001)
36. Y.Y. Keum, H.N. Li, Phys. Rev. D **63**, 074 006 (2001)
37. BaBar Collaboration, hep-ex/0508046
38. A.J. Buras, R. Fleischer, S. Recksiegel, F. Schwab, Nucl. Phys. B **697**, 133 (2004)
39. A. Kagan, Phys. Lett. B **601**, 151 (2004)
40. J.M. Cornwall, Phys. Rev. D **26**, 1453 (1982)
41. J.M. Cornwall, J. Papavasiliou, Phys. Rev. D **40**, 3474 (1989)
42. J.M. Cornwall, J. Papavasiliou, Phys. Rev. D **44**, 1285 (1991)
43. R. Alkofer, L. von Smekal, Phys. Rep. **353**, 281 (2001)
44. L. von Smekal, R. Alkofer, A. Hauck, Phys. Rev. Lett. **79**, 3591 (1997)
45. D. Zwanziger, Phys. Rev. D **69**, 016 002 (2004)
46. D.M. Howe, C.J. Maxwell, Phys. Lett. B **541**, 129 (2002)
47. R. Alkofer, Phys. Rev. D **70**, 014 002 (2004)
48. A.C. Aguilar, A.A. Natale, P.S. Rodrigues da Silva, Phys. Rev. Lett. **90**, 152 001 (2003)
49. S. Furui, H. Nakajima, AIP Conf. Proc. **717**, 685 (2004)
50. S. Brodsky, S. Menke, C. Merino, J. Rathsman, Phys. Rev. D **67**, 055 008 (2003)

51. A.C. Mattingly, P.M. Stevenson, Phys. Rev. D **49**, 437 (1994)
52. M. Baldicchi, G.M. Prosperi, Phys. Rev. D **66**, 074008 (2002)
53. R.E. Cutkosky, J. Math. Phys. **1**, 429 (1960)
54. G. Buchalla, A.J. Buras, M.E. Lautenbacher, Rev. Mod. Phys. **68**, 1125 (1996)
55. W.F. Palmer, Y.L. Wu, Phys. Lett. B **350**, 245 (1995)
56. M. Beneke, M. Neubert, Nucl. Phys. B **675**, 333 (2003)
57. M. Beneke et al., Nucl. Phys. B **606**, 245 (2001)
58. S.W. Bosch, G. Buchalla, Nucl. Phys. B **621**, 459 (2002)
59. M. Beneke, T. Feldmann, D. Seidel, Nucl. Phys. B **612**, 25 (2001)
60. J.F. Sun, G.H. Zhu, D.S. Du, Phys. Rev. D **68**, 054003 (2003)
61. S.B. Shalom, G. Eilam, Y.D. Yang, Phys. Rev. D **67**, 014007 (2003)
62. Y.D. Yang, F. Su, G.R. Lu, H.J. Hao, Eur. Phys. J. C **44**, 243 (2005)
63. A.G. Williams et al., hep-ph/0107029 and references therein
64. C.D. Lu, K. Ukai, M.Z. Yang, Phys. Rev. D **63**, 074009 (2001)
65. S. Eidelman et al., Phys. Lett. B **592**, 1 (2004)
66. C.H. Chen, H.N. Li, Phys. Rev. D **63**, 014003 (2001)
67. J. Zhu, Y.L. Shen, C.D. Lü, Phys. Rev. D **72**, 054015 (2005)
68. Y.L. Wu, Int. J. Mod. Phys. A **18**, 5363 (2003) [hep-th/0209021]
69. Y.L. Wu, Mod. Phys. Lett. A **19**, 2191 (2004) [hep-th/0311082]
70. H.Y. Cheng, K.C. Yang, Phys. Lett. B **511**, 40 (2001)
71. H.Y. Cheng, K.C. Yang, Phys. Rev. D **64**, 074004 (2001)
72. M. Beneke, T. Feldmann, Nucl. Phys. B **592**, 3 (2001)
73. S. Descotes-Genon, C.T. Sachrajda, Nucl. Phys. B **625**, 239 (2002)
74. P. Ball, V.M. Braun, Nucl. Phys. B **543**, 201 (1999)